J Mol Model (2014) 20:2461
DOI 10.1007/s00894-014-2461-8

ORIGINAL PAPER

The effect of HNS on the reinforcement of TNT crystal: a molecular simulation study

Wen Qian · Yuanjie Shu · Huarong Li · Qing Ma

Received: 29 June 2014 / Accepted: 2 September 2014 / Published online: 20 September 2014
© Springer-Verlag Berlin Heidelberg 2014

Abstract The effect of crystal modifier 2,2',4,4',6,6'-hexanitrostillbene(HNS) on the reinforcement of crystalline 1,3,5-trinitrotoluene (TNT) was investigated by molecular simulation. The intermolecular interactions between HNS and TNT were revealed by quantum chemistry calculations in detail, strong attractive forces were found between HNS and TNT. The solid interface models of TNT/HNS along three crystalline directions were studied, the distance between HNS molecule and TNT system was narrowed after optimization; the mechanical properties were calculated, showing the mechanism of the reinforcement.

Keywords 2,2',4,4',6,6'-hexanitrostillbene(HNS) · Intermolecular interaction · 1,3,5-trinitrotoluene(TNT) · Mechanical property

Introduction

1,3,5-Trinitrotoluene(TNT)-based melt-cast explosive is a kind of widely-used composite explosive[1]. The toughness test of the explosive showed that the physical nature of TNT is fragile [2], the intermolecular interaction in TNT crystal is weak and the anisotropy of thermal expansion is obvious, which induce micro cracks for TNT-based explosive parts during heating cycling, and affect the sensitivity and charging properties [3]. Portnoy et al. [4] analyzed the reason for TNT's weak mechanical property, and the crystallography of TNT was considered to be the main reason. Experiments show that when 2,2',4,4',6,6'-hexanitrostillbene(HNS) was added into the composite explosive, the mechanical property of TNT crystal can be enhanced. Trevino [5], Parry [6, 7], and Cartwright et al. [8] carried out experimental investigations to validate the positive effect of HNS on TNT crystal, however, the mechanism of the intermolecular interactions was not discussed.

Recently molecular simulation methods such as quantum chemistry (QC), molecular mechanics (MM), molecular dynamics (MD), and so on were applied in the field of composite explosives [9]. The intermolecular interactions between different explosive molecules can be calculated and analyzed in detail; Li et al. [10] had investigated the intermolecular interactions between explosive 1,3,5-trinitrobenzene(TNB) and 1,3,5-triamino-2,4,6-trinitrobenzene(TATB) by QC method at PM3 level, and the interaction energies were calculated; Niu et al. [11] studied the intermolecular interactions between TNT and 1,3,5-trinitro-1,3,5-triazacyclohexane(RDX)by density functional theory (DFT) method at B3LYP/6-31G(d) level, and the detonation properties were calculated theoretically; Our group investigated the energetic systems N-methyl-N'-nitroguanidine (MeNQ) - ammonium nitrate (AN) [12] and 2,4,6,8,10,12-hexanitro- 2,4,6,8,10,12-hexaazaisowurtzitane(CL-20)/TNT co-crystal [13, 14], DFT and MD methods were used to investigate the intermolecular interactions and mechanical properties. In this paper, QC and MD methods were applied to investigate the effect of HNS on TNT crystal, the intermolecular interactions were analyzed, and the mechanism of the reinforcement of TNT crystal was discussed.

W. Qian · H. Li · Q. Ma
Institute of Chemical Materials, China Academy of Engineering Physics, Mianyang 621900, China

Y. Shu (✉)
Xi'an Modern Chemistry Research Institute, Xi'an 710065, China
e-mail: syjfree@sohu.com

Q. Ma
Department of Chemistry, Nanjing University of Science and Technology, Nanjing 210094, China

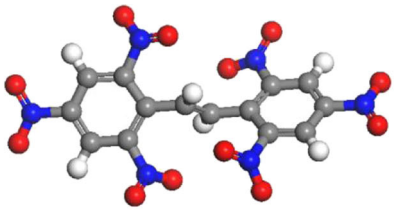

(a)

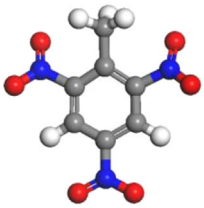

(b)

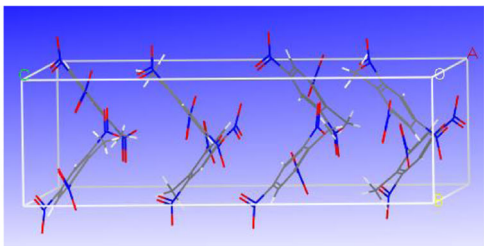

(c)

Fig. 1 Structures of HNS and TNT (**a**) Molecular structure of HNS; (**b**) Molecular structure of TNT; (**c**) Crystal structure of TNT

Simulation and calculation details

Molecular modeling

The molecular configuration of HNS was constructed in Materials Studio Modeling [15], as shown in Fig. 1a. The TNT molecule (Fig. 1b) and crystalline TNT (Fig. 1c) were constructed according to the experimental data [16] from Cambridge Crystallographic Data Center (CCDC), the crystal belongs to P_{ca21} space group, with cell parameters $a=1.4911$ nm, $b=0.6077$ nm, $c=2.0017$ nm, $\alpha=\beta=\gamma=90°$. It was obvious that HNS has a very similar molecular configuration with TNT, just like two TNT molecules added together head by head.

Quantum chemistry calculations

The QC calculations were carried out in Dmol^3 program [17, 18] at GGA/PBE [19] level [with an exchange-correction function of Perdew-Burke-Emzerhof (PBE) form under generalized gradient approximation (GGA)], the double-numeric-quality (DNP) basis set and dispersion-corrected density functional theory (DFT-D) correction were used. Structures of HNS molecule as well as two stable trimers consisted of one HNS molecule and two TNT molecules (HNS-2TNT a,b) [6–8] were constructed and optimized. Then hydrogen-bond (H-bond) interactions of HNS-2TNT were examined. Energy and property calculations were performed, and the corrected total energies were obtained. The intermolecular interaction energies can be calculated from the total

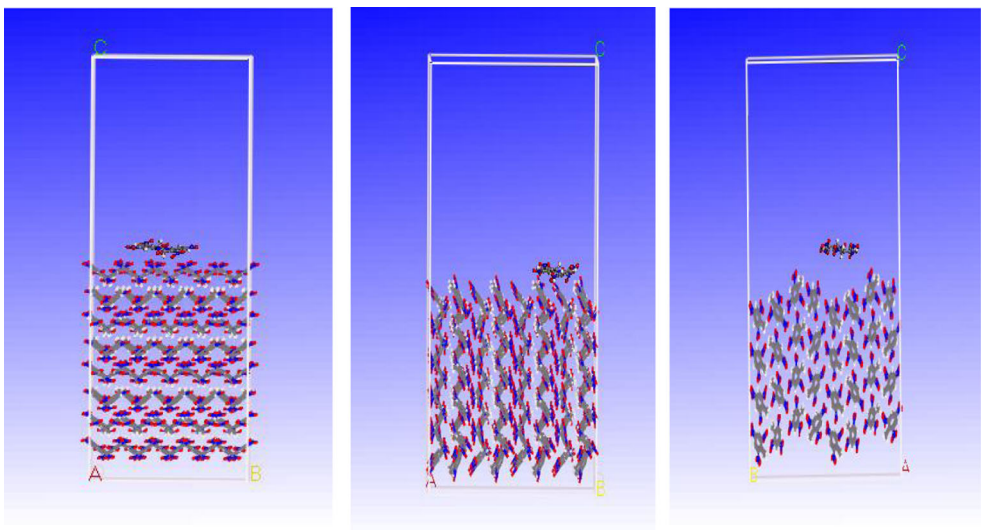

（a） （b） （c）

Fig. 2 Solid interface model of HNS on crystalline TNT (**a**) along TNT (0 0 1); (**b**) along TNT (0 1 0);(**c**) along TNT (1 0 0)

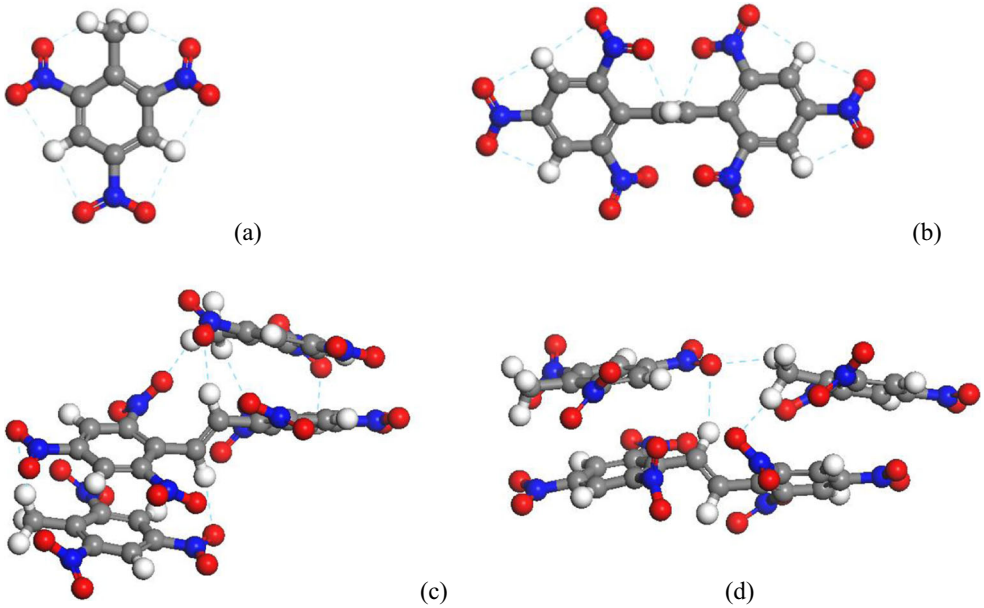

Fig. 3 Hydrogen bonds (shown in light blue) in HNS, TNT, and two optimized configurations of HNS-2TNT trimer (**a**) Intramolecular H-bonds in TNT; (**b**) intramolecular H-bonds in HNS; (**c**) intermolecular H-bonds in HNS-2TNT a; (**d**) intermolecular H-bonds in HNS-2TNT b

energies of TNT, HNS and the HNS-2TNT by the simplified equation [20] as:

$$E_{\text{inter}} = E_{\text{complex}} - (2E_{\text{TNT}} + E_{\text{HNS}}), \quad (1)$$

where E_{inter} is the interaction energy, E_{TNT}, E_{HNS} and E_{complex} are the total energies (kJ mol^{-1}) of the TNT molecule, the HNS molecule and HNS-2TNT respectively.

The molecular electrostatic potential (ESP) is the potential energy of a proton at a particular location near a molecule [21], the ESPs of HNS as well as HNS-2TNT were examined based on the QC calculations. Negative electrostatic potential(colored in shades of blue) corresponds to attraction of the proton by the concentrated electron density in the molecules, while positive electrostatic potential(colored in shades of red) corresponds to repulsion of the proton by the atomic nuclei in regions where low electron density exists and the nuclear charge is incompletely shielded.

Molecular dynamics simulations

In order to investigate the reinforcement of the modifier along each TNT crystalline direction, a 2×5×2 TNT supercell was

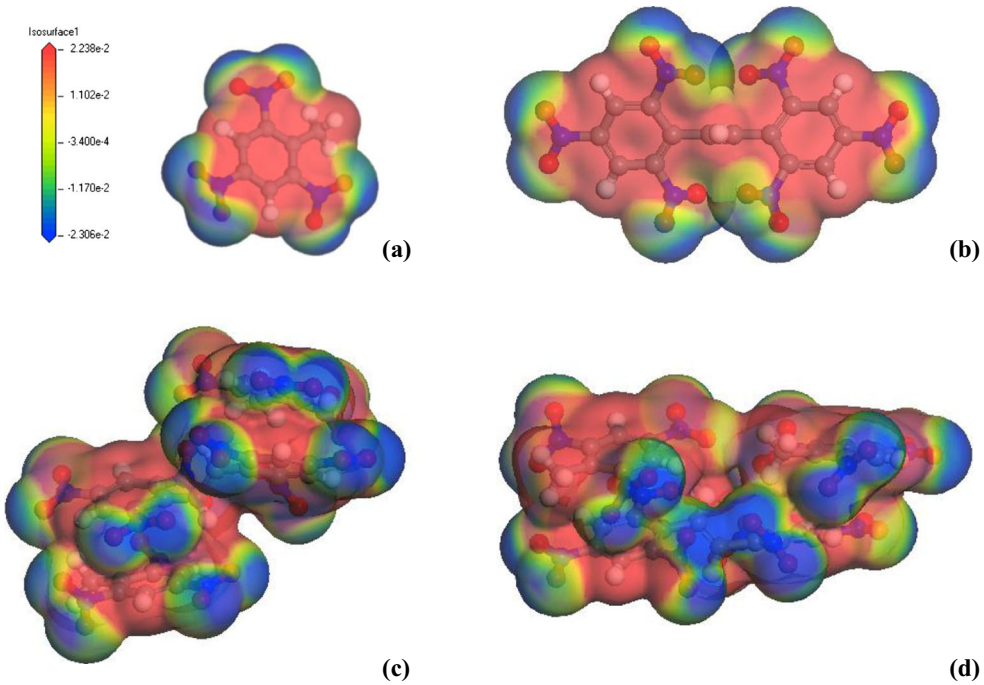

Fig. 4 Electrostatic potentials of HNS and HNS-2TNT (**a**) TNT [13]; (**b**)HNS molecule; (**c**)HNS-2TNT a;(**d**)HNS-2TNT b Red: positive electrostatic potential; blue: negative electrostatic potential (between $2.283 \cdot 10^{-2}$ and $-2.036 \cdot 10^{-2}$ Hartree)

Table 1 Inteaction energies in HNS-2TNT using DFT-D correction

System	E_{TNT} [kJ/mol]	E_{HNS} [kJ/mol]	$E_{complex}$ [kJ/mol]	E_{inter} [kJ/mol]
HNS-2TNT a	−2322206.208	−4638179.385	−9282862.861	271.060
HNS-2TNT b	−2322206.208	−4638179.385	−9282832.481	240.680

Note: E_{TNT}, E_{HNS} and $E_{complex}$ are molecular energies of TNT, HNS and the complex, respectively. E_{inter} is intermolecular interaction energy.

constructed based on the TNT primitive cell. Then the supercell was cleaved along three different crystal faces (1 0 0), (0 1 0) and (0 0 1). The optimized HNS molecule was put in three different boxes which have periodic boundary condition, and each box has a basal face the same as each cleaved TNT supercell. Then each box was combined with the matched cleaved TNT supercell to build the TNT/HNS interface model as shown in Fig. 2. The structures were optimized by molecular mechanics and energy-minimized.

Then MD simulations were performed on the optimized structures under constant particle number, pressure, and temperature (NPT) ensemble with condensed-phase optimized molecular potential for atomistic simulation studies (COMPASS) [22, 23] force field, and the validation of the force field was confirmed in previous studies [13, 14, 24]. To simulate the normal condition, the target temperature and pressure were set to 298 K and 100 kPa, Anderson method [25] was used to control the temperature and Berendsen method [26] was used to control the pressure. Initial velocity was sampled by Maxwell distribution, and velocity Verlet arithmetic [27] was utilized. Van der Waals force was calculated by atom-based method, and coulomb interaction was calculated by Ewald method [28, 29]. Each MD simulation lasted 200 ps to ensure the system properly equilibrated both in energy and temperature, and the time step was 1 fs.

The equilibrium trajectory documents were selected to perform the mechanical property calculations. Optimization process was carried out before the calculation. The elastic constants were obtained by the mechanical analysis, and then other mechanical parameters could be calculated. The generalized Hooke's law is often written as:

$$\sigma_i = C_{ij}\varepsilon_j, \tag{2}$$

where σ_i is the stress tensor (GPa), ε_j is the strain tensor(GPa), and C_{ij} is the 6×6 stiffness matrix of elastic constants. If the material is idealized as an isotropic material, the stiffness matrix of the stress–strain behavior can be fully described by specifying only two independent coefficients (Lamé coefficients) as:

$$\begin{bmatrix} \lambda+2\mu & \lambda & \lambda & 0 & 0 & 0 \\ \lambda & \lambda+2\mu & \lambda & 0 & 0 & 0 \\ \lambda & \lambda & \lambda+2\mu & 0 & 0 & 0 \\ 0 & 0 & 0 & \mu & 0 & 0 \\ 0 & 0 & 0 & 0 & \mu & 0 \\ 0 & 0 & 0 & 0 & 0 & \mu \end{bmatrix}, \tag{3}$$

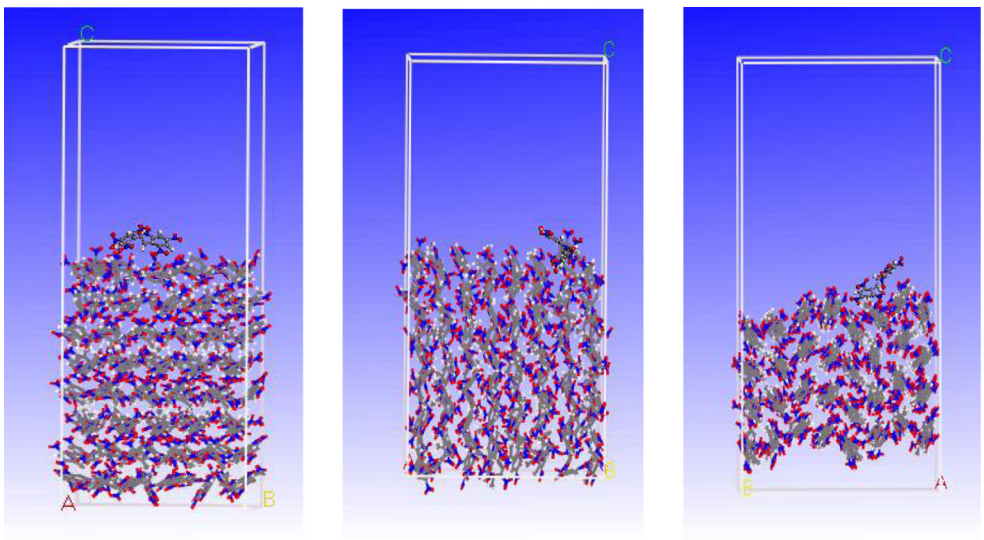

(a) (b) (c)

Fig. 5 Solid molecular structures of TNT/HNS after MD simulation (**a**) along TNT (0 0 1); (**b**) along TNT (0 1 0); (**c**) along TNT (1 0 0)

Table 2 Elastic constants [GPa] of pure TNT and solid-state TNT/HNS at normal condition

Systems	TNT	TNT/HNS (0 0 1)	TNT/HNS (0 1 0)	TNT/HNS (1 0 0)
C_{11}	61.711	58.195	58.828	57.291
C_{22}	39.811	36.332	36.624	36.107
C_{33}	47.159	46.135	46.010	46.524
C_{44}	14.147	11.133	11.047	11.485
C_{55}	4.919	7.769	7.007	7.649
C_{66}	19.419	13.506	13.071	13.560
C_{12}	30.173	21.332	21.625	21.107
C_{13}	27.046	20.135	21.010	20.524
C_{14}	0.194	−0.133	−0.047	−0.485
C_{15}	0.109	0.077	−0.070	0.649
C_{16}	−0.010	−0.151	0.071	−0.560
C_{23}	40.097	31.792	31.435	31.538
C_{24}	−0.025	−0.147	0.039	−0.471
C_{25}	−0.050	0.171	−0.085	0.805
C_{26}	−0.010	0.006	0.114	−0.675
C_{34}	−0.011	−0.024	−0.138	−0.745
C_{35}	0.086	0.260	0.007	0.821
C_{36}	−0.004	0.072	−0.046	−0.922
C_{45}	−0.002	0.133	0.152	0.124
C_{46}	0.024	0.272	0.545	−0.190
C_{56}	−0.006	0.044	0.475	−0.019

where λ and μ are the Lamé coefficients. For the isotropic case, the familiar elastic modulus can be written in terms of the Lamé coefficients as follows:

$$\begin{cases} E = \mu\left(\dfrac{3\lambda + 2\mu}{\lambda + \mu}\right) \\ K = \lambda + \dfrac{2}{3}\mu \\ G = \mu \\ \gamma = \dfrac{\lambda}{2(\mu + \lambda)} \end{cases}, \tag{4}$$

wherein E is Young's modulus (GPa), K is Bulk modulus (GPa), G is Shear modulus (GPa), and γ *is* Poisson's ratio respectively [30, 31].

Results and discussion

Configurations and hydrogen bond

Figure 3 shows the two optimized configurations of HNS-2TNT (one HNS molecule with two TNT molecules according to the literatures [6–8]). The hydrogen bonds in these systems were shown. It can be seen that intramolecular H-bonds exsit in HNS and TNT molecules (in Fig. 3a, b), which will improve the molecular stability; and intermolecular H-bonds exsit between HNS and TNT as well as two TNT molecules (Fig. 3c,d), which will enhance the attractive interactions between the molecules and improve the stability of the trimers [32].

Electrostatic potentials

The ESPs of TNT (Fig. 4a) had been investigated in our previous study [13], compared with the ESPs of HNS (Fig. 4b), we can find that the electrons concentrate around the nitrogen group ($-NO_2$), and the blue in the electrostatic potentials associated with the negative regions of nitro oxygen(O)s [21], which is the same as that of TNT. The potentials of the trimers (Fig. 4c,d) are shown to give a comparison with the potentials of HNS and TNT separately, it can be seen that the red regions hold together and overlapped to form a stable complex. In addition, it can be seen that the benzene rings of HNS and TNT stack face to face, because the benzene rings of both HNS and TNT have extra π-electrons, the attractive non-covalent π-π stackings exist between aromatic rings of HNS and TNT molecules.And these π-π conjugation interactions between the benzene rings contribute to the stability of the trimer as well [33].

Intermolecular interaction energy

The intermolecular interaction energies were calculated (Table 1) by Eq. (1). For both configurations, relatively strong attractive forces exist between HNS and TNT. The force of attraction between HNS and TNT is the result of the combined effect of van del Waals forces, hydrogen-bonds, and electrostatic interactions.

Table 3 Mechanical properties of pure TNT and solid-state TNT/HNS at normal condition

Systems	TNT	TNT/HNS (0 0 1)	TNT/HNS (0 1 0)	TNT/HNS (1 0 0)
Young's modulus (E)[GPa]	34.004	29.095	28.055	29.328
Bulk modulus (K)[GPa]	32.457	31.622	31.607	31.655
Shear modulus (G)[GPa]	12.828	10.803	10.375	10.898
Poisson's ratio (γ)	0.325	0.347	0.352	0.346

Interface interaction

During the optimization and MD simulation process, the distance between TNT system and HNS was narrowed, proving the existence of relatively strong attractive forces between HNS and TNT. Equilibrium TNT/HNS structures are shown in Fig. 5, it can be found that the attractive forces exist along each crystalline direction.

Accordingly, intermolecular interactions esxisting between HNS and TNT are stonger than just van del Waals forces, which help to form a stable complex of HNS-2TNT, and also make HNS absorb on the TNT crystal face more easily to prevent the TNT crystal from growing too fast, so that more tiny crystal particles can form to reduce the internal stress in composite explosives [4–8].

Mechanical properties

The mechanical property calculation and analysis were carried out on the equilibrium structures, and the elastic constants (C_{ij}, GPa) of pure TNT and interface model TNT/HNS at normal condition along each crystal face were obtained. The results are shown in Table 2.

It can be seen that in the elastic constants matrix, all diagonal elements C_{ii} and the off-diagonal elements C_{12}, C_{13}, C_{23} are larger than other elements, and the other elements are almost zero, which indicate considerable anisotropy of the systems. The elements can be divided into three groups: C_{11}, C_{22}, C_{33}; C_{44}, C_{55}, C_{66}; C_{12}, C_{13}, C_{23}. Compared to pure TNT, the differences in each group of TNT/HNS's elements are narrowed slightly; the equalization of C_{ij} indicates that the addition of the TNT-like HNS molecule will improve the isotropy of the composite explosive [20].

The mechanical parameters of pure TNT and solid-state TNT/modifier at normal condition along each crystal face were calculated and compared, the Young modulus (E,GPa), bulk modulus (K,GPa), shear modulus (G,GPa), and Poisson's ratios (γ) are shown in Table 3.

The mechanical properties of TNT/HNS along each crystal face were compared to that of pure TNT. It was found that the moduli are reduced when adding HNS molecule, indicating the attenuation of stiffness, the reinforcement of elasticity and the reduction of brittleness [20]. The Poisson's ratios of TNT/HNS are all in the range of plastics 0.2∼0.4, which indicates that the composite explosive will show good plasticity and will be easy to be machined. In addition, the properties along different crystalline faces are not so different, showing improvements along each direction. It can be conclude that HNS has positive effects on the mechanical reinforcement of TNT crystal.

Conclusions

Molecular simulations and calculations were carried out to investigate the effect of HNS on TNT crystal. The results are as follows.

(1) Quantum chemistry analysis showed that strong attractive forces exist between HNS and TNT because of intermolecular hydrogen-bonds, electrostatic potentials and π-π conjugation interactions.
(2) The interface models of TNT/HNS along different crystal faces were investigated, during the optimizations and MD simulations, the distance between HNS and TNT molecules was narrowed in each direction.
(3) MD simulations and mechanical property calculations were carried out on the solid molecular models, mechanical parameters were obtained, proving improvement of the isotropy and the reinforcement of the mechanical property.

The consequences show the mechanism of the reinforcement of TNT crystal by HNS, which indicates that TNT modifiers need to have a TNT-like structure, strong interactions with TNT, and better mechanical property to improve the properties of the TNT crystal. The conclusion is helpful in the design of reinforcing modifiers for TNT-based composite explosives.

Acknowledgments The authors acknowledge the support of NSAF Fund (Grant No.11076002) and NSFC Fund (Grant No.51373159). The computation resources in the Simulation Center of CAEP are appreciated.

References

1. Shu YJ, Huo JC (2011) Introduction to explosives. Chemical Industry Press, Beijing
2. Smith DL, Thorpe BW (1973) J Mater Sci 8:757–759
3. Ma Q, Shu YJ, Luo G, Chen L, Zheng BH, Li HR (2012) Toughening and elasticizing route of TNT based melt cast explosives. Chin J Energ Mater 20(5):618–629
4. Portnoy S, Livingston NJ (1982) Production of fine-grained cast charges with unoriented crystal structure of TNT or explosive compositions containing TNT. US4360394
5. Trevino SF, Portnoy S, Choi CS (1979) Effects of HNS on Cast TNT. ARLCD-MR-79001
6. Parry MA, Thorpe BW (1978) Nucleation and growth of TNT containing HNS. MRL-R-708
7. Parry MA, Thorpe BW (1979) The effective nucleant during the grain modification of TNT with HNS. MRL-R-748
8. Cartwright M, Hill CJ (1995) Thermal investigation of the crystallization nucleant formed between HNS and TNT. J Therm Anal 44: 1021–1036
9. Qian W, Shu YJ (2013) Progress of computer simulation for intermolecular interactions in composite explosive. Chin J Energ Mater 21(5):629–637

10. Li JS, Xiao HM, Dong HS (2000) A study on the intermolecular interaction of energetic system-mixtures containing -CNO2 and -NH2 groups. Prop Explos Pyrotech 25(1):26–30
11. Niu XQ, Zhang JG, Feng XJ, Chen PW, Zhang TL, Wang SY, Zhang SW, Zhou ZN, Yang L (2011) Theoretical investigation on intermolecular interactions between the ingredients TNT and RDX of composition B. Acta Chim Sinica 69(14):1627–1638
12. Chen L, Li HR, Xiong Y, Xu RJ, Xu T, Liu XF, Shu YJ (2012) Structure and molecular interaction of methyl-nitroguanidine and hydrazine nitrate eutectics. Chin J Energ Mater 20(5):560–564
13. Li HR, Shu YJ, Chen L, Ma Q, Ju XH (2013) Theoretical insights into the nature of intermolecular interactions in TNT/CL-20 cocrystal and its properties. Proceedings of the 16th Seminar on New Trends in Research of Energetic Materials, Pardubice, Czech Republic, 742–753
14. Li HR, Shu YJ, Gao SJ (2013) Easy methods to study the smart energetic TNT/CL-20 co-crystal. J Mol Model 19(11): 4909–4917
15. Accelrys Software Inc (2012) Materials Studio Release Notes, Release 6.1. Accelrys Software Inc, San Diego
16. Carper WR, Davis LP, Extine MW (1982) Molecular structure of 2,4, 6-trinitrotoluene. J Phys Chem 86:459
17. Delley B (1990) J Chem Phys 92:508
18. Delley B (2000) J Chem Phys 113:7756
19. Perdew JP, Burke K, Ernzerhof M (1996) Generalized gradient approximation made simple. Phys Rev Lett 77:3865–3868
20. Qiu L, Xiao H (2009) Molecular dynamics study of binding energies, mechanical properties, and detonation performances of bicyclo-HMX-based PBXs. J Hazard Mater 164:329–336
21. Murray JS, Politzer P (2011) The electrostatic potential: an overview. WIREs Comp Mol Sci 1:153–163
22. Sun H (1998) COMPASS: an ab initio forcefield optimized for condensed-phase applications — overview with details on alkane and benzene compounds. J Phys Chem B 102:7338
23. Sun H, Ren P, Fried JR (1998) The COMPASS forcefield: parameterization and validation for polyphosphazenes. Comput Theor Polym Sci 8:229
24. Rigby D, Sun H, Eichinger BE (1998) Computer simulations of poly (ethylene oxides): forcefield, PVT diagram and cyclization behavior. Polym Int 44:311–330
25. Andersen HC (1980) Molecular dynamics simulations at constant pressure and/or temperature. J Phys Chem 72:2384
26. Berendsen HJC, Postma JPM, van Gunsteren WF, DiNola A, Haak JR (1984) Molecular dynamics with coupling to an external bath. J Chem Phys 81:3684–3690
27. Verlet L (1967) Computer experiments on classical fluids. I. Thermodynamical properties of Lennard-Jones molecules. Phys Rev 159:98–103
28. Ewald PP (1921) Die Berechnung optischer und elektrostatischer Gitter potentiale (The calculation of optical and electrostatic lattice potentials). Ann Phys Leipzig 64:253
29. Karasawa N, Goddard WA (1989) Acceleration of convergence for lattice sums. J Phys Chem 93:7320–7327
30. Watt JP, Davies GF, O'Connell RJ (1976) The elastic properties of composite materials. Rev Geophys Space Phys 14:541–563
31. Weiner JH (1983) Statistical mechanics of elasticity. Wiley, New York
32. Beijer FH, Kooijman H, Spek AL, Sijbesma RP, Meijer EW (1998) Self-complementarity achieved through quadruple hydrogen bonding. Angew Chem Int Ed 37(1–2):75–78
33. Hunter CA, Sanders JKM (1990) The nature of π-π interactions. J Am Chem Soc 112(14):5525–5534